

INVESTIGATING THE IMPACT OF METTL16 CELLULAR LOCALIZATION ON RNA BINDING PREFERENCES

by

Daniel Joel Nance

A Senior Honors Project Presented to the

Honors College

East Carolina University

In Partial Fulfillment of the

Requirements for

Graduation with Honors

by

Daniel Joel Nance

Greenville, NC

May, 2019

Approved by:

Dr. Kyle D. Mansfield

Department of Biochemistry and Molecular Biology, ECU Brody School of Medicine

## **ABSTRACT**

Recently, mRNA modification by N6-methyladenosine (m6A) has been shown to be involved in post-transcriptional regulation processes including mRNA stability, splicing and promotion of translation. Accordingly, the mRNA methylation complex of Mettl3/14/WTAP has been the subject of intense study. However, we and others have also identified Mettl16 as an RNA m6A methyltransferase that can methylate both coding and noncoding RNAs, but its biological role remains unclear. Mettl16's RNA targets have been identified and include the long noncoding RNA MALAT1, the snRNA U6, as well as many mRNAs including MAT2A, HIF1, and SEMA4F. To investigate the functional role of Mettl16 we knocked out Mettl16 via CRISPR but were unable to obtain viable clones suggesting that it may be essential for cell growth; a finding supported by the literature. Transient knockdown via siRNA was successful, but no effect on RNA target expression or translation was observed. We are currently developing a tetracycline inducible METTL16 knockdown system to examine the effects of more long-term depletion. We have been successful at overexpressing METTL16 and identifying additional RNA targets by immunoprecipitation. Interestingly, when overexpressing exogenous Mettl16 we have observed differences from the endogenous protein in both the RNA targets as well as the relative affinity for targets. We hypothesize that this difference may be related to cellular localization as the endogenous protein appears to be mainly cytoplasmic while a significant fraction of the overexpressed protein is nuclear. Thus, while METTL16 has been asserted to be a nuclear protein, our findings depict METTL16 as a primarily cytoplasmic methyltransferase that may alter its RNA binding preferences depending on its cellular localization. Future studies will seek to confirm differences between cytoplasmic and nuclear RNA targets in addition to exploring the physiological role of Mettl16 through long-term knockdown.

## INTRODUCTION

Methylation on the sixth position of the sugar moiety of adenosine ( $m^6A$ ) is one of the most common mRNA modifications, and it has been shown to affect all aspects of post-transcriptional regulation including mRNA stability, maturation, and translation (Zhao et al., 2017). Methyltransferase like -3 and -14 (METTL3 and METTL14) and Wilms' tumor associating protein (WTAP) make up the mRNA  $m^6A$  methyltransferase complex, which uses a S-adenosyl methionine (SAM) binding domain on METTL3 to target specific mRNAs for methylation (Liu et al., 2016; Ping et al., 2014). SAM is used as a substrate for methylation of mRNAs with a RRACH  $m^6A$  consensus sequence, which is usually in the 3' UTR (Liu et al., 2016). The YTH family of proteins modulate the effects of  $m^6A$ , as YTHDF1 has been shown to increase translation of  $m^6A$  containing mRNA, while YTHDF2 directs mRNA degradation (Zhao et al., 2017).  $m^6A$  has been shown to play a role in embryonic stem cell differentiation, circadian rhythms, and cancer. Recently, the Mansfield lab has discovered a role for  $m^6A$  in the hypoxic response, where increased  $m^6A$  activity has been linked to hypoxic conditions and stabilization of a subset of hypoxia-related mRNAs (Fry et al., 2017).

In the last two years, Mettl16 has been identified as an RNA  $m^6A$  methyltransferase that can methylate both coding and noncoding RNAs. Primarily, Mettl16 has been shown to methylate the U6 snRNA (Warda et al, 2017). It can also bind and methylate the long noncoding RNAs MALAT1 and XIST (Brown et al, 2016; Pendleton et al, 2017). Mettl16 has been shown to bind and methylate many mRNAs, including MAT2A, which can regulate its alternative splicing in response to cellular SAM levels (Pendleton et al, 2017). Furthermore, a recent global analysis suggests that RBM3, STUB1, and HIF-1 $\alpha$  pre-mRNA are also Mettl16 targets (Warda et al, 2017).

Perhaps the most intriguing aspect of Mettl16 m<sup>6</sup>A activity is the importance of structure when binding targets, not just sequence like the METTL3/METTL14/WTAP complex. Mettl16 m<sup>6</sup>A methylation of MAT2A is reliant upon a conserved hairpin (hp1) for binding and that same sequence and structure is required for U6 methylation as well, but interestingly, is not found in other Mettl16 targets (Pendleton et al, 2017). In *in vitro* methylation studies, Mettl16 appears to prefer stem loop structures with the methylated adenosine being unpaired in a single stranded loop or bulge (Mendel et al, 2018). Additionally, instead of the heterodimeric “writer” complex formed by METTL3/METTL14 m<sup>6</sup>A methyltransferase, Mettl16 functions as a homodimer (Ruszkowska et al, 2018). This homodimeric Mettl16 is necessary for binding the MALAT1 triple helix, although monomeric Mettl16\_291, which contains only the methyltransferase domain, is sufficient for methylating U6 and MAT2A RNAs (Pendleton et al, 2017).

At a molecular level, the effects of Mettl16 m<sup>6</sup>A activity are best understood in the context of cellular S-adenosylmethionine (SAM) levels and intron retention of MAT2A mRNA. SAM is a methyl donor for most cellular methylation reactions, and is created using SAM synthetases that convert methionine and ATP into SAM (Pendleton et al, 2017). In human cells, the SAM synthetase is encoded by the MAT2A gene and is expressed in all cell types except liver cells. Methionine depletion stabilizes MAT2A mRNA, which has six hairpin structures in its 3' UTR that serve as binding sites for Mettl16. When SAM levels are high intracellularly, Mettl16 binds the hp1 of MAT2A RNA, methylates it, and quickly dissociates to support intron retention. Intron retention targets the MAT2A mRNA for nuclear degradation. Low intracellular levels of SAM do not allow for efficient methylation by Mettl16, increasing Mettl16 occupancy on the mRNA which results in increased splicing of the retained intron. This increases stabilization and translation of the MAT2A mRNA and production of SAM synthetase which

increases SAM levels in the cell. Additionally, the YTHDC1 m<sup>6</sup>A “reader” protein may play a role in processing the mature MAT2A mRNA and monitoring intracellular SAM levels (Shima et al, 2017).

The physiological significance of Mettl16 is largely unknown at this point, although its role in maintaining cellular SAM levels is vital for cell proliferation (Shima et al, 2017). The frequent presence of Mettl16 frameshift mutations in colorectal cancers suggests that it may act as a tumor suppressor but that has not been formally tested (Yeon et al, 2017). Interestingly, whole mouse Mettl16 knockout results in blastocysts that are unfit to develop further and abort, although the reason for this is not definitively known (Mendel et al, 2018). Thus, Mettl16 appears to be essential for mammalian life, even though its physiological role remains speculative at best.

These findings indicate that Mettl16 is an important protein in human cells, despite its status as an understudied m<sup>6</sup>A methyltransferase. We want to further explore its methylation targets, how Mettl16 expression levels affect its binding preferences, and determine the effects of Mettl16 methylation at the cellular and organismal levels.

## RESULTS

### *Mettl16 Knockdown and Effects on Literature Targets*

We first attempted to determine the physiological role of METTL16 by knocking it out using CRISPR, but we were unable to create stable cell lines (Data Not Shown). We then sought Mettl16 knockdown using two siRNA's (7 and 9) in HEK293T cells over the course of 72 hours. Western blotting confirmed that compared to the negative control siRNA, treatment with Mettl16 siRNA, either individually, or combined together, resulted in significant knockdown of Mettl16 expression (Figure 1A). Real-time PCR was then used to assess RNA expression of Mettl16 targets from the literature. As shown in Figure 1B, while there was a slight increase in the mRNA expression of HIF-1alpha, so significant effects were seen for any of the literature targets. Thus, we concluded that short-term knockdown of Mettl16 by siRNA may not be sufficient to show physiological effects. To investigate whether siRNA knockdown of Mettl16 was sufficient to alter its methylation activity, the RNA was also analyzed for m<sup>6</sup>A levels via LCMS. As shown in Figure 2, similar levels of m<sup>6</sup>A were seen in either total RNA or polyA selected mRNA from control and Mettl16 knockdown cells, suggesting again that siRNA knockdown of Mettl16 is not sufficient to elicit a physiological effect. We are currently developing a Tetracycline (Tet)-inducible shRNA knockdown model to provide long-term knockdown of Mettl16. HEK293T cells stably transfected with two different Tet-inducible shRNA constructs showed Doxycycline (Dox) dependent knockdown of Mettl16 protein levels after either 6 or 10 days (Figure 3). It is our hope that this system will now allow us to deplete Mettl16 levels to an extent that will affect m<sup>6</sup>A levels and provide a model in which to determine its physiological role.

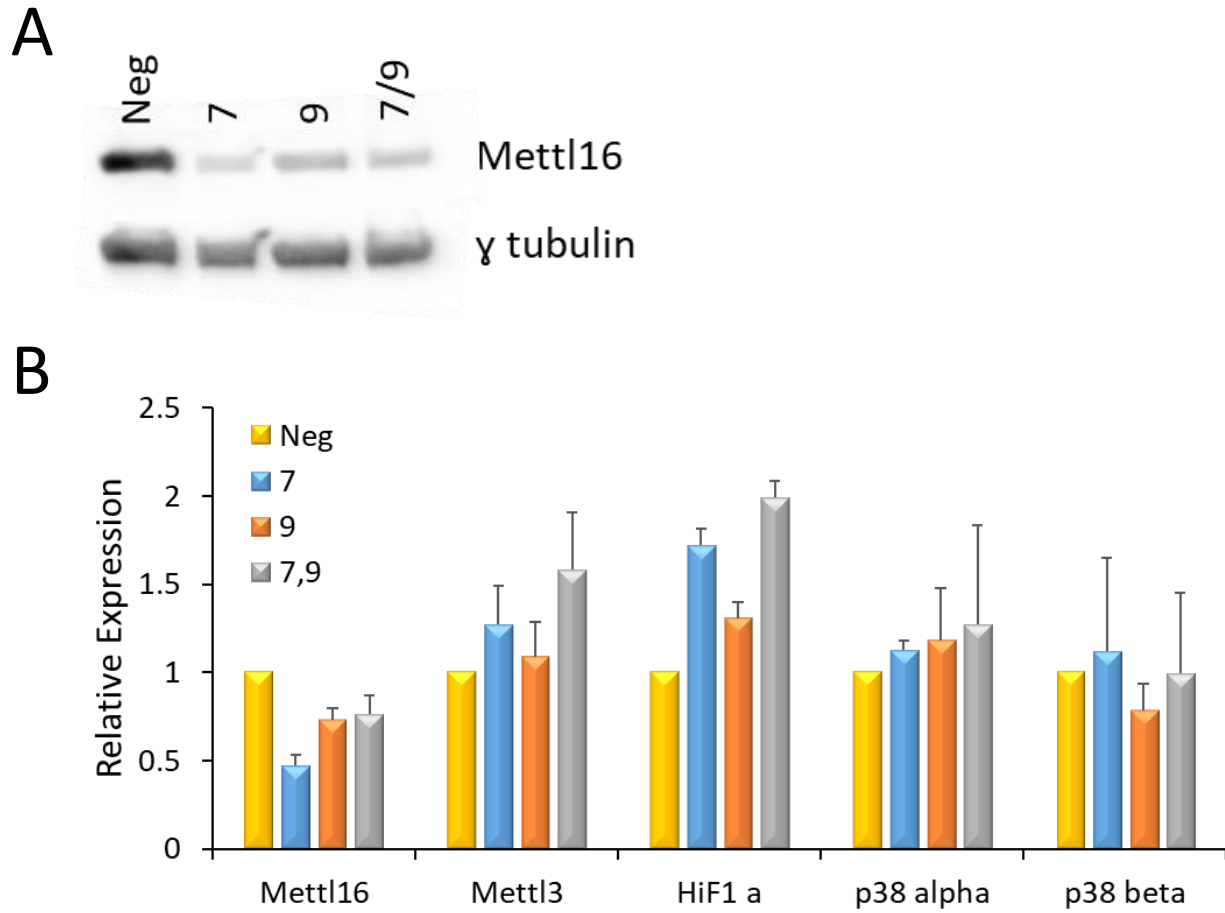


**Figure 1: Effect of Mettl16 knockdown on mRNA expression.** Mettl16 protein was knocked down for 72 hours using two siRNAs (7 & 9) in HEK293T cells as confirmed by western blot (Figure 1A). Real-time PCR (Figure 1B) was used to examine the effect on literature-based Mettl16 target mRNAs.

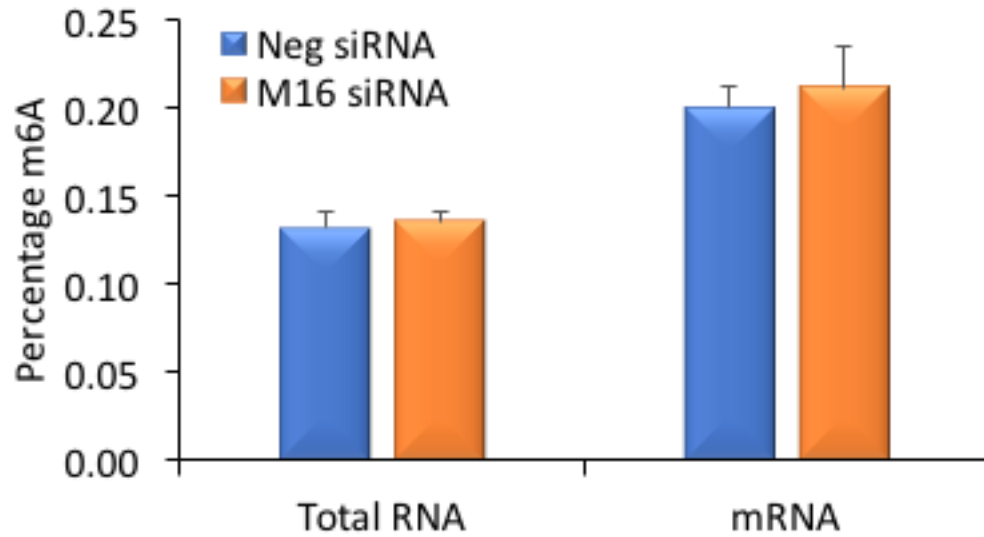


**Figure 2: Effect of Mettl16 knockdown on m<sup>6</sup>A levels.** Liquid Chromatography-Mass Spectrometry (LC-MS) was used to determine how m<sup>6</sup>A levels change when Mettl16 was knocked down using siRNA.

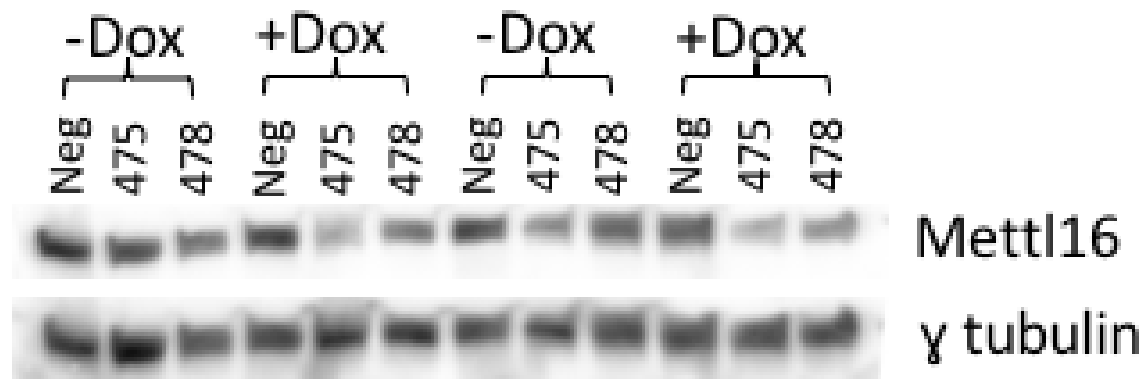


**Figure 3: Effect of shRNA Knockdown on Mettl16 Expression.** Mettl16 knockdown using a stable HEK293T line containing tetracycline-inducible Mettl16 shRNA constructs (475, 478) as shown by western blot. When treated with Doxycycline, Mettl16 levels decrease with both constructs.  $\gamma$  tubulin was used as a loading control.

### *Identification of Mettl16 Binding Targets*

To confirm Mettl16 literature targets and identify new targets, HEK293T cells were stably transfected with either FLAG-GFP, FLAG-Mettl3, or FLAG-Mettl16 overexpression constructs. Cell extracts were then immunoprecipitated with FLAG magnetic beads. Western blotting was used to confirm successful immunoprecipitation as evidenced by depletion of the expected band in the supernatant and enrichment in the IP (Figure 4A). RNA was also extracted, and real-time PCR used to measure fold enrichment of Mettl16 targets Real-Time PCR (Figure 4B). Samples were corrected for input levels and then fold enrichment of the target in the Mettl16 IP compared to the GFP IP was calculated. As shown in Figure 4B, U6 snRNA appears to be the primary binding target of Mettl16, although other RNAs such as MAT2A, B2M, and Malat1 were also targets. Importantly, U2 snRNA, which is not known to harbor an m6A, served as a negative control and exhibited very little enrichment in the Mettl16 IP.

To determine if these targets were the same for endogenous Mettl16, we also performed an immunoprecipitation for endogenous Mettl16 (Figure 5A). Western blotting confirmed that the IP was successful with Mettl16 protein remaining in the supernatant of the negative IP while being depleted from the Mettl16 antibody supernatant and appearing in the IP lane. Real-Time PCR was again used to measure RNA enrichment of targets relative to the normal rabbit serum (NRS) control, after normalizing for input levels (Figure 5B). Interestingly, in contrast to the FLAG-Mettl16 immunoprecipitation, MAT2A mRNA appeared to be the primary target of endogenous Mettl16, although U6 snRNA was still a target. Additional mRNAs such as Myc, NTSDC2, and Sema4F as well as 18S rRNA were also identified as potential Mettl16 targets while 5S rRNA and U1 and U2 snRNA appear to not be bound by Mettl16, which is expected given that they are not known to be methylated.

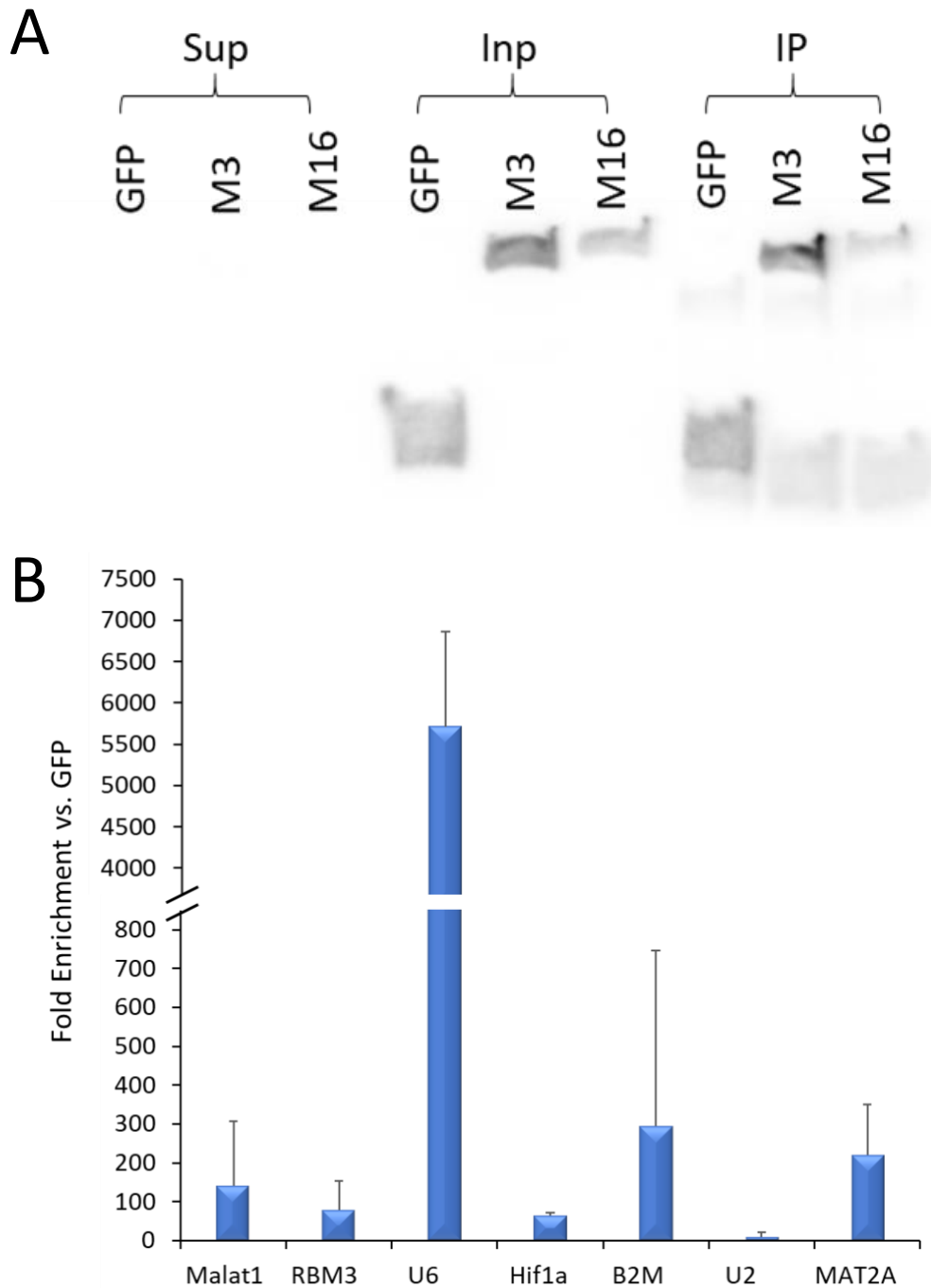


**Figure 4: Identification of FLAG-Mettl16 targets.** FLAG-Mettl16 protein was stably overexpressed and immunoprecipitated from HEK293T cells as confirmed by western blot (Figure 4A) and associated RNAs isolated via Trizol. Real-time PCR (Figure 4B) was used to identify targets showing enrichment over FLAG green fluorescent protein (GFP) control immunoprecipitation (IP). U6 snRNA was the primary binding target (Figure 4B), but mRNA's like B2M, Malat1, and MAT2A were also bound by Mettl16.

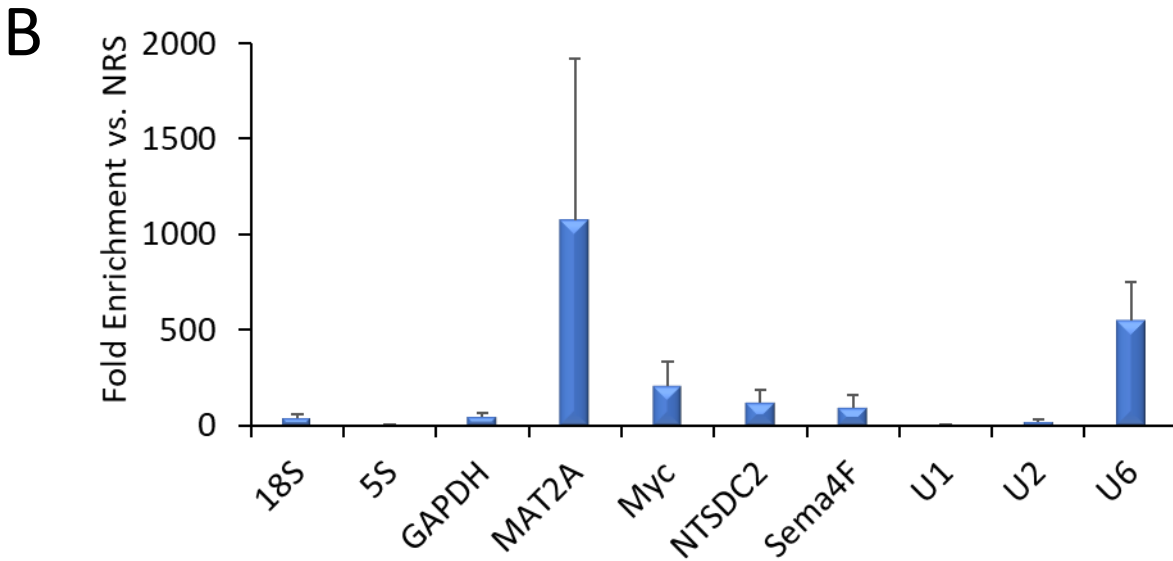
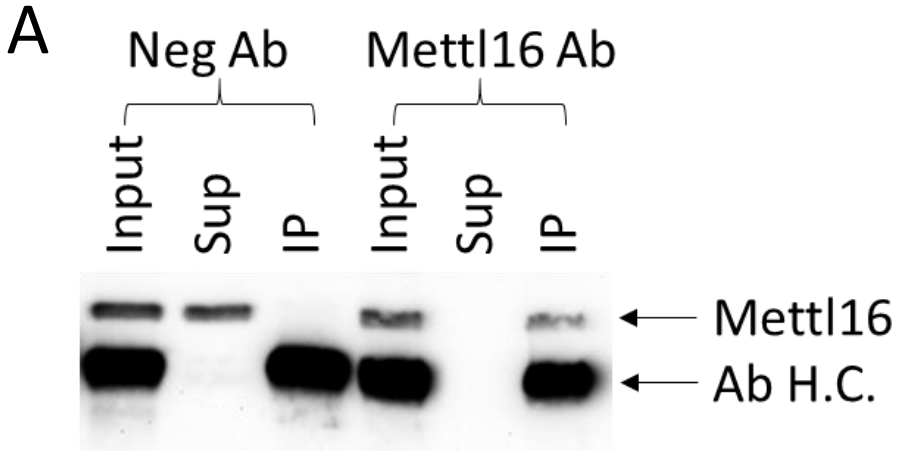


**Figure 5: Identification of Endogenous Mettl16 Targets.** Mettl16 protein was immunoprecipitated from HEK293T cells as confirmed by western blot (Figure 5A). Real-time PCR (Figure 5B) was used to identify targets showing enrichment over normal rabbit serum (NRS) negative IP. U6 snRNA was still a strong target, but MAT2A mRNA was the primary binding target of endogenous Mettl16.

### *Investigation of Mettl16 Cellular Localization*

Based on the differences in targets between exogenous and endogenous Mettl16, we theorized that Mettl16 localization may change based on expression levels and that this may impact target selection. Biochemical fractionation of FLAG Mettl16 overexpressing HEK293T cells revealed that Mettl16 was found mainly in the cytoplasm, with small amounts also found in the nucleus and outer nuclear envelope (ONE) fractions (Figure 6A). Lamin and LDH served as markers for nuclear and cytoplasmic fractions respectively and confirm successful fractionation with little to no contamination. This contrasts with current literature characterizing Mettl16 as a predominately nuclear protein. To investigate whether overexpression was affected Mettl16 cellular localization we also analyzed endogenous Mettl16's localization in HEK293T cells using biochemical fractionation (Figure 6B). Compared to the FLAG-overexpressed Mettl16 (Figure 6A) much more endogenous Mettl16 was found in the cytoplasm relative to the nucleus. These results suggest that overexpression of Mettl16 does indeed affect its cellular localization and that this may underly the differences in RNA targets seen in the immunoprecipitations.

To confirm the cellular localization of Mettl16, we examined its localization in two cell lines in which Mettl16 has been reported to be nuclear. As shown in Figure 7, in both HEK293 and HELA cells, Mettl16 appears to be predominately located in the cytoplasm. We also examined Mettl16's localization in a series of MCF10 breast cancer cells representing different stages of breast cancer progression. MCF10A's represent immortalized, yet non-tumorigenic cells. AT1's are transformed but are weakly tumorigenic, while the Ca1h line represents a highly aggressive tumorigenic cell line. Again, we saw Mettl16 primarily in the cytoplasm in all three of these cell lines (Figure 8), confirming our belief that Mettl16 is a cytoplasmic protein.

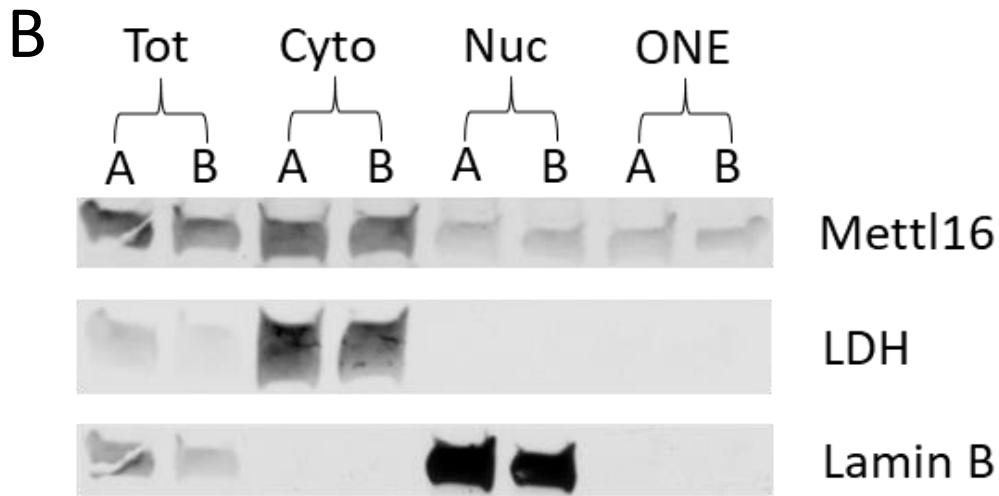
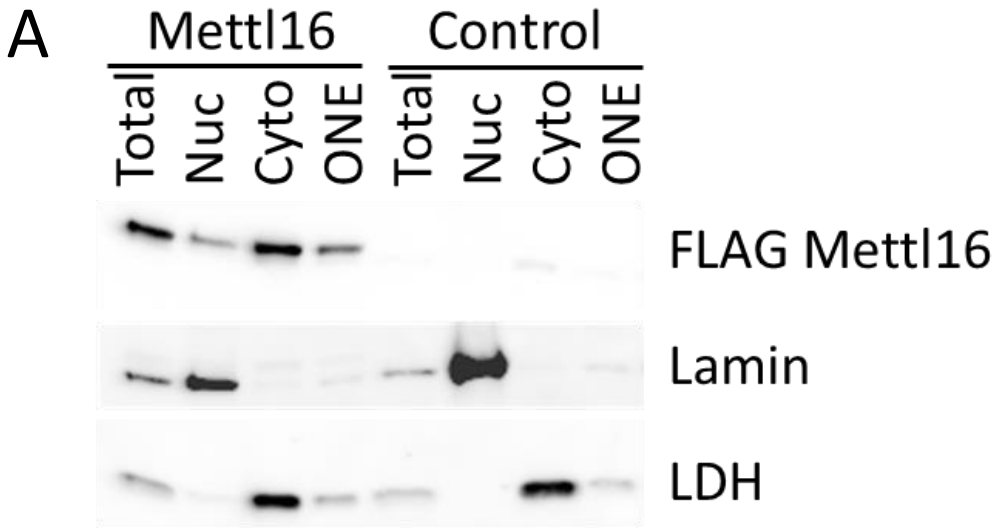


**Figure 6: Identification of Mettl16 Cellular Localization in HEK293T Cells.** Extracts from HEK293T cells stably expressing FLAG-Mettl16 were separated into Nuclear (Nuc), Cytoplasmic (Cyto), and Outer Nuclear Envelope (ONE) fractions and subjected to western blot to determine Mettl16 cellular localization (Figure 6A). FLAG-Mettl16 was primarily located in the cytoplasm, with small amounts in the ONE and nuclear fractions. Lamin was used as a nuclear control, and LDH was a cytoplasmic control. Biochemical cellular fractionation was also used to determine the location of endogenous Mettl16 protein in multiple cell lines including replicate (A,B) HEK293T samples (Figure 6B).



**Figure 7: Identification of Mettl16 Cellular Localization in HEK293 and HELA Cells.**

Extracts from HEK293 and HELA cells were separated into Nuclear (N), Cytoplasmic (C), and Outer Nuclear Envelope (O) fractions and subjected to western blot to determine Mettl16 cellular localization. Lamin was used as a nuclear control, and LDH was a cytoplasmic control. The same results were seen as in Figure 6B, with Mettl16 located almost exclusively in the cytoplasm.

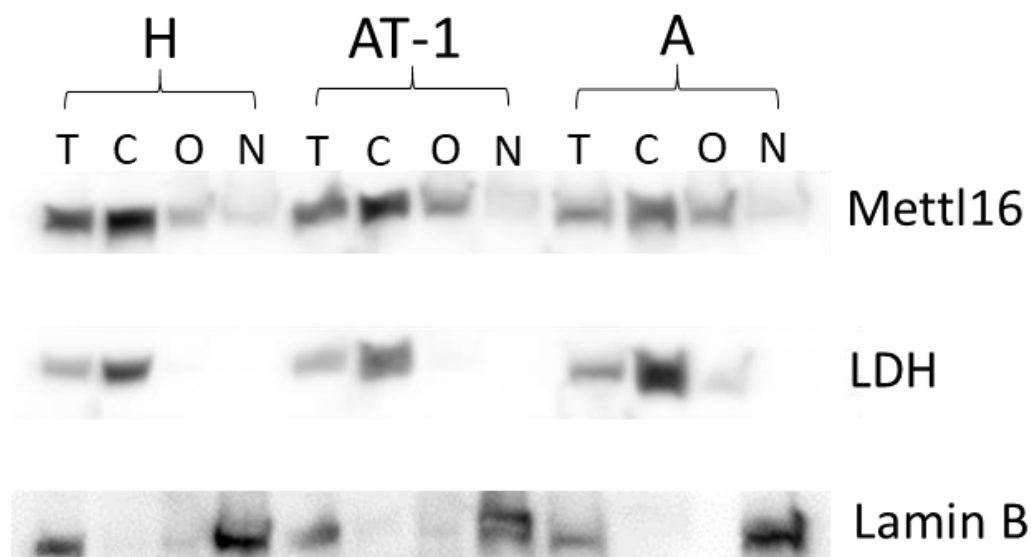


**Figure 8: Identification of Mettl16 Cellular Localization in MCF-10 Lines.** Extracts from three MCF-10-derived breast cancer lines were subjected to western blot to determine Mettl16 cellular localization (H=MCF10-Ca1h, AT-1=MCF10-AT1, A=MCF10-A; T=Total, C=Cytoplasmic, O=Outer Nuclear Envelope, N=Nuclear). Lamin was used as a nuclear control, and LDH was a cytoplasmic control. The same results were seen as in Figure 6B, with Mettl16 located almost exclusively in the cytoplasm.

## DISCUSSION

Short-term knockdown of Mettl16 protein levels using siRNAs was effective, but no functional effect on target levels was apparent from these studies (Figure 1B). We propose that functional effects of Mettl16 knockdown may require longer than 72 hours to become apparent, so short-term knockdown may not be sufficient to study cellular effects of different Mettl16 expression levels. This may be due to the long-lived nature of Mettl16's noncoding RNA targets such as U6, although that has not been examined. Since creation of a CRISPR Mettl16 knockout clone was unsuccessful (Data Not Shown), it appears that Mettl16 is necessary for cell survival. This supports previous reports which were unable to generate Mettl16 knockout cells (Wang 2015, Pendleton et al, 2017) and is in line with a recent report suggesting that Mettl16 was essential for the growth of a number of cancer cell lines (Barbieri, 2017). Thus, we have created a Tet-inducible long-term Mettl16 knockdown system that will hopefully allow us to study the effects of persistent Mettl16 deprivation (Figure 3). We will use this system in future studies to examine the effects of Mettl16 knockdown on target RNA and protein levels, as well as cellular growth and proliferation.

Our FLAG-Mettl16 immunoprecipitation (Figure 4B) indicates that U6 snRNA is the definitive primary binding target of Mettl16, and other mRNAs like MAT2A, B2M, and MALAT1 are secondary targets of Mettl16. This disputes the belief that mRNAs and lncRNAs are significant binding targets (Shima et al, 2017; Brown et al, 2016). However, the endogenous Mettl16 immunoprecipitation (Figure 5B) suggests that MAT2A is the primary binding target, and U6 is only a moderately strong binding target. The clear difference in binding preference based on levels of cellular Mettl16 expression indicates that some aspect of the overexpression is changing how or where this binding occurs.

This change in target preference made us question whether expression levels were impacting METTL16 cellular localization and in turn modulating its binding preferences depending on cellular location. We used biochemical cellular fractionation to determine where endogenous Mettl16 resides (Figure 6B) and found it mainly in the cytoplasm, although small amounts were also found in the nucleus. This contradicts the current characterization of Mettl16 as a nuclear m<sup>6</sup>A methyltransferase (Brown et al, 2016; Warda et al, 2017), although those studies utilized immunohistochemistry in other cell types. To confirm cytoplasmic localization of Mettl16, we decided to pursue cell types used in those previous studies. We performed a biochemical cellular fractionation on both HELA and HEK293 cells (Figure 7), again finding that Mettl16 resides primarily in the cytoplasm. Three additional cell types were also fractionated (Figure 8) and these all support our finding that Mettl16 is predominantly a cytoplasmic protein with limited nuclear activity. Interestingly, we also saw significant amounts of the Mettl16 target U6 snRNA in the cytoplasm (Data Not Shown), which also contradicts current understandings that U6 is an exclusively nuclear snRNA. Future studies will focus on identifying the cellular compartment in which Mettl16 binds and methylates U6 snRNA and other targets, especially given that many of the mRNA methylation sites appear to reside in introns of pre-mRNA (Pendleton et al, 2017) which again should be exclusively nuclear.

Mettl16 is essential for mammalian life based on our attempts at creating CRISPR Mettl16 knockouts (Data Not Shown) and previous knockout studies in mice embryos (Mendel et al, 2018). The reason for its essentiality is unclear, but we believe that it plays two major roles in cellular development and survival. Previous studies suggest that Mettl16's regulation of MAT2A mRNA levels via the SAM synthetase pathway affects developmental events (Mendel et al, 2018). Mettl16 knockout downregulates MAT2A mRNA levels, which causes the

production of blastocysts that are not capable of further development. We also believe that Mettl16's strong preference for binding U6 snRNA is important for proper functionality of the spliceosome complex. m<sup>6</sup>A methylation of U6 may be important to its development, and the lack of this modification could have global effects on splicing that result in production of incorrect proteins and eventual cell death.

Our future studies will focus on creating Mettl16 gene variants with localization sequences that force the protein to either the nucleus or cytoplasm. These variants can be used to determine the binding preferences of Mettl16 based on its localization, which may explain the differences we have seen in past studies. Also, we plan to use the Tet-inducible Mettl16 knockdown system (Figure 3) to study molecular and physiological effects of long-term Mettl16 knockdown. This can be used to confirm previously identified targets, and potentially uncover new ones as well. We hope that elucidating the physiological function of Mettl16 in humans will allow us to better understand its role in disease and provide avenues for future treatments to target.

## REFERENCES

- Barbieri, I., Tzelepis, K., Pandolfini, L., Shi, J., Millán-Zambrano, G., Robson, S. C., . . . Kouzarides, T. (2017). Promoter-bound METTL3 maintains myeloid leukaemia by m6A-dependent translation control. *Nature*, *552*(7683), 126-131.
- Brown, J. A., Kinzig, C. G., DeGregorio, S. J., & Steitz, J. A. (2016). Methyltransferase-like protein 16 binds the 3'-terminal triple helix of MALAT1 long noncoding RNA. *Proc Natl Acad Sci U S A*, *113*(49), 14013-14018.
- Fry, N. J., Law, B. A., Ilkayeva, O. R., Holley, C. L., & Mansfield, K. D. (2017). N6-methyladenosine is required for the hypoxic stabilization of specific mRNAs. *Rna*, *23*(9), 1444-1455.
- Liu, K., Ding, Y., Ye, W., Liu, Y., Yang, J., Liu, J., & Qi, C. (2016). Structural and Functional Characterization of the Proteins Responsible for N(6)-Methyladenosine Modification and Recognition. *Curr Protein Pept Sci*, *17*(4), 306-318.
- Mendel, M., Chen, K., Homolka, D., Gos, P., Pandey, R. R., Mccarthy, A. A., & Pillai, R. S. (2018). Methylation of Structured RNA by the m6A Writer METTL16 Is Essential for Mouse Embryonic Development. *Molecular Cell*, *71*(6), 986-1000.
- Pendleton, K. E., Chen, B., Liu, K., Hunter, O. V., Xie, Y., Tu, B. P., & Conrad, N. K. (2017). The U6 snRNA m(6)A Methyltransferase METTL16 Regulates SAM Synthetase Intron Retention. *Cell*, *169*(5), 824-835 e814.
- Ping, X. L., Sun, B. F., Wang, L., Xiao, W., Yang, X., Wang, W. J., . . . Yang, Y. G. (2014). Mammalian WTAP is a regulatory subunit of the RNA N6-methyladenosine methyltransferase. *Cell Res*, *24*(2), 177-189.
- Shima, H., Matsumoto, M., Ishigami, Y., Ebina, M., Muto, A., Sato, Y., . . . Igarashi, K. (2017). S-Adenosylmethionine Synthesis Is Regulated by Selective N6-Adenosine Methylation and mRNA Degradation Involving METTL16 and YTHDC1. *Cell Reports*, *21*(12), 3354-3363.
- Wang, T., Birsoy, K., Hughes, N.W., Krupczak, K.M., Post, Y., Wei, J.J., Lander, E.S., and Sabatini, D.M. (2015). Identification and characterization of essential genes in the human genome. *Science* *350*, 1096–1101.
- Warda, A. S., Kretschmer, J., Hackert, P., Lenz, C., Urlaub, H., Hobartner, C., . . . Bohnsack, M. T. (2017). Human METTL16 is a N(6)-methyladenosine (m(6)A) methyltransferase that targets pre-mRNAs and various non-coding RNAs. *EMBO Rep*, *18*(11), 2004-2014.
- Yeon, S. Y., Jo, Y. S., Choi, E. J., Kim, M. S., Yoo, N. J., & Lee, S. H. (2017). Frameshift Mutations in Repeat Sequences of ANK3, HACD4, TCP10L, TP53BP1, MFN1, LCMT2, RNMT, TRMT6, METTL8 and METTL16 Genes in Colon Cancers. *Pathology & Oncology Research*, *24*(3), 617-622.
- Zhao, B. S., Roundtree, I. A., & He, C. (2017). Post-transcriptional gene regulation by mRNA modifications. *Nat Rev Mol Cell Biol*, *18*(1), 31-42.

## **METHODS**

**Tissue Culture:** HEK293T cells were maintained in DMEM with 4g/L Glucose, 10% FBS, and 1X Pen/Strep at 37°C, 5% CO<sub>2</sub>.

**Knockdown and Overexpression of Mettl16:** For knockdown, HEK293T cells were transfected with 20 μM siRNA (Life Technology Silencer Select) targeting Mettl16 or a negative control siRNA with Lipofectamine. For overexpression, 2 μg of plasmid expressing a FLAG tagged Mettl16, Mettl3, GFP Control or pcDNA 3.1 were used. Cells were transfected for 24 to 72 hours before harvesting to allow for sufficient knockdown/overexpression of Mettl16.

**Western Blots:** Whole-cell lysates were prepared in whole-cell extract buffer (WCEB: 50 mM Tris pH 7.4, 150 mM NaCl, 5 mM EDTA, 0.1% SDS, and complete protease inhibitor [Promega]). Equal amounts of protein (30–50 μg) were electrophoresed on a mini-PROTEAN any KD acrylamide gel (Bio-Rad Laboratories) and transferred to Hybond ECL nitrocellulose (GE Healthcare). The blot was blocked with 5% non-fat dry milk (LabScientific) in Tris-buffered saline with 0.1% Tween 20 (TBST) for 1 h at room temperature, followed by primary antibody in blocking buffer overnight at 4°C. After washing extensively with TBST, blots were incubated for 1–2 h at room temperature with appropriate HRP-linked secondary antibody (GE Healthcare), washed again with TBST, developed using Bio-Rad Clarity Western ECL Substrate (Bio-Rad Laboratories), and imaged via MYECL Imager (Thermo Scientific).

**RNA Extraction:** Trizol (Life Technologies) was used for all RNA extractions according to the manufacturer's protocol. RNA was further purified and treated with RNase-Free DNase I (Life

Technologies) using the PureLink RNA Mini Kit (Life Technologies). For RNA extraction from ribonucleoprotein immunoprecipitations (RNP-IP) and sucrose gradients, GlycoBlue (Life Technologies) was added as a carrier during the precipitation step. RNA quality and quantity were determined via NanoDrop 1000 (ThermoFisher Scientific).

**PCR:** Reverse transcription was performed on 1  $\mu$ g of total RNA in a 20  $\mu$ l reaction with the iScript cDNA synthesis kit (Bio-Rad Laboratories, 170-8891). After diluting cDNA five-fold, quantitative real-time PCR was performed using a Roche Lightcycler 96 with Fast Start Essential DNA Green (Roche Diagnostics Corporation, 06-924-204-001) and primers from Integrated DNA Technologies, Inc. Primer efficiency was verified to be over 95% for all primer sets used. Quantification of mRNA was carried out via  $\Delta\Delta$ CT analysis using GAPDH mRNA and the respective control condition for normalization. All real-time PCR primer sets were designed so the products would span at least one intron (>1kb when possible), and amplification of a single product was confirmed by agarose gel visualization and/or melting curve analysis.

**LC-MS/MS of RNA for nucleoside modification analysis:** Purified RNA was digested to individual nucleosides and modified nucleosides were quantified as previously described (Gokhale et al. 2016). Briefly, digestion was performed with nuclease P1 (Sigma, 2U) in buffer containing 25 mM NaCl and 2.5 mM ZnCl<sub>2</sub> for 2 h at 37°C, followed by incubation with Antarctic Phosphatase (NEB, 5U) for an additional 2 h at 37°C. Nucleosides were then separated and quantified at the Duke Molecular Physiology Institute using UPLC-MS/MS.

**FLAG Immunoprecipitation of Mettl16:** Beads labeled with FLAG Antibody (Sigma) were washed and resuspended in NT2 supplemented with DTT, RNase Out and 0.5M EDTA. Cells were harvested in 250 $\mu$ l PLB and equal amounts of lysate were added to each IP and tumbled for 4 hours at 4°C. After washing, beads were lysed in Trizol (RNA) or WCEB with protease inhibitors (protein). Relative enrichment of RNA in the IP was determined by comparing to input via the  $\Delta$ CT method.

**Endogenous Immunoprecipitation of Mettl16:** Cells were harvested in PLB (100 mM KCl, 5 mM MgCl<sub>2</sub>, 10 mM HEPES (pH 7.0), 0.5% NP40, 1 mM DTT, 100 units/ml RNase Out, with Protease inhibitor cocktail). Beads labeled with FLAG Antibody (Sigma) or normal rabbit serum (NRS) were washed and resuspended in NT2 (50 mM Tris-HCl (pH 7.4), 150 mM NaCl, 1 mM MgCl<sub>2</sub>, 0.05% NP40) supplemented with 1 mM DTT, 100 units/ml RNase Out and 20mM EDTA. Equal amounts of lysate were added to each IP and tumbled for 4 hours at 4°C. After washing, beads were lysed in Trizol (RNA) or WCEB (protein). Fold enrichment was determined via the  $\Delta\Delta$ CT method using GapDH and the NRS IP for normalization.

**Cell Fractionation:** Cells were resuspended in a hypotonic buffer (10 mM NaCl, 10 mM Tris-HCl, pH 7.4, 1.5 mM MgCl<sub>2</sub> with PI) and allowed to swell for 5 minutes. Lysis was achieved by vortexing for 2-3 seconds and nuclei were pelleted at 1,000 g for 5 minutes at 4°C. The supernatant was removed and stored as cytoplasmic fraction. The outer nuclear envelope was removed by washing nuclei in the above buffer containing 1% NP40 and 0.5% sodium deoxycholate. The supernatant after centrifugation was designated ONE. The nuclear pellet was sonicated in lysis buffer containing 0.1% SDS.